SUPRA-SUBDUCTION ORIGIN OF THE NIDAR OPHIOLITIC SEQUENCE, INDUS SUTURE ZONE, LADAKH, INDIA: EVIDENCE FROM MINERAL CHEMISTRY OF UPPER MANTLE ROCKS

Himanshu K. Sachan

Wadia Institute of Himalayan Geology, Dehra Dun-248001, India (e-mail: petrology@sancharnet.in).

Keywords: *Mineral chemistry, SSZ Ophiolite, Nidar Ophiolite. Ladakh, India.*

ABSTRACT

The ultramafic rocks of Nidar ophiolitic sequence in the eastern part of the Ladakh (NW Himalaya) have been studied combining petrography and mineral chemistry data. The ultramafic rocks mainly consist of spinel-harzburgite and spinel-dunite, that are intruded by spinel-bearing pyroxenites. The modal and chemical composition of minerals in harzburgite indicates a strongly-depleted nature consistent with a residual origin after the extraction of basaltic melt by single or multiple partial melting events. In contrast, dunite was probably formed as a consequence of interaction between harzburgite and migrating melt(s), after the partial melting events. This is well corroborated by the petrographical and chemical evidence, e.g., the growth of secondary mineral aggregates and the large chromite component in the spinels.

The mineral chemistry suggests that the melts percolating and interacting with harzburgite were rich in MgO and NiO and deficient in CaO, Al_2O_3, and TiO_2. In particular, the low Ti content shown by clinopyroxenes and spinels (which are cumulus phases in pyroxenites and secondary neoblastic phases in peridotites), in association with high Cr# (> 60) exhibited by all the spinels, are consistent with parent melt of boninitic affinity. These melts are typical of island arc environment. Therefore, this infers that the ultramafic units of Nidar ophiolite underwent melt percolation in a supra-subduction tectonic environment related to fore-arc setting.

INTRODUCTION

Over all in the earth's crust, ophiolites are the major components in the realm of subduction related tectonic environment. The study of pillow lavas and mantle sequence in the ophiolites can give impetus to advance our knowledge on the magma generation and its extraction from the mantle (Beccaluva and Serri, 1988; Hebert and Laurent, 1989; Ohnenstetter et al., 1990; Orberger et al., 1995). The well-studied ophiolitic sequence of Oman, Cyprus, Thailand and Philippines indicated that they were formed in supra-subduction set-up (Auge and Roberts, 1982; Greenbaum, 1977; Orberger et al., 1995). Till date no proper attention have been paid on Indus Suture ophiolites in the western Himalaya in order to understand the processes involved in the genesis of ultramafic melts from upper mantle.

The Indus Suture Zone represents a junction between the Indian Plate and the Karakoram-Tibetan block of the Eurasian Plate. It extends to the North of Himalaya from East to West for about 2500 km (Thakur and Mishra, 1984) and is characterized by the presence of ophiolitic sequences, ophiolitic mélanges, plutonic-volcanic rock association of magmatic arc, flysch and molasses (Thakur, 1981; Honegger et al., 1982). The dismembered portion of ultramafic rock mixed with sediments and blueschists occurs in the western as well as in eastern part of the Ladakh, i.e. Shergol and Zildat ophiolitic mélange (Thakur and Mishra, 1984; Honegger et al., 1989). Furthermore, the eastern part of the Ladakh is still geologically unexplored. Along the Indus Suture Zone, a complete ophiolitic sequence is exposed only in the eastern part of the Ladakh, which is known as Nidar ophiolitic sequence (Virdi, 1986; Fig. 1). This sequence is sandwiched between the Tso Morari Crystalline Complex to the South and the Indus Formation to the North.

The aim of this study is to provide constraints on its geodynamic significance and to understand the petrochemical processes involved in the building of subduction complex in the Himalayan regon.

OPHIOLITIC SEQUENCE

In the Indus Suture Zone only the Nidar area in the Eastern Ladakh exhibits a full lithologic spectrum of typical ophiolitic sequence. The ophiolite is composed of three zones; 1) Ultramafics; 2) Gabbro and pillow lava; 3) chert interbedded with volcanics (Fig. 1). The age of this ophiolitic sequence is dated to be Cretaceous, on the basis of the fossil assemblage present in the chert unit (Virdi, 1986).

The ultramafic zone comprises spinel-harzburgite and spinel-dunite, and is 8 to 10 km wide in the Nidar-Kyon Tso section. Spinel-harzburgite is present at the base of the sequence, whereas spinel-dunite occupies the upper level, in tectonic contact with the mafic rocks (Fig. 1). The spinel-dunite hosts minor amount of chromite either in the form of disseminated grains (about 2-4 mm) or veins. Pyroxenite is present in the form of centimeter to meter sized sills either in dunite or harzburgite.

To the North, the ultramafic association is overlain by gabbros. Some dolerite dykes are also encountered within this zone, but a real sheeted dyke complex is absent in the Nidar ophiolitic sequence. Pillow lavas (volcanics) are observed to the North of the gabbro zone. They consist of basic to intermediate volcanics (T. Ahmad, Personal Communication.) with pillow structure of around 0.5 to 1 m across. The uppermost pillow unit is layered containing volcanics interbedded with greenish, radiolarian-rich, chert. The red chert represents the uppermost unit of the ophiolitic sequence, and it is 100-200 m thick (Fig. 2). The northern limit of Nidar ophiolitic sequence is marked by southwards dipping thrust with Indus formation, whereas the southern limit is marked by northwards dipping thrust with Tso Morari Crystalline (Thakur and Mishra, 1984).

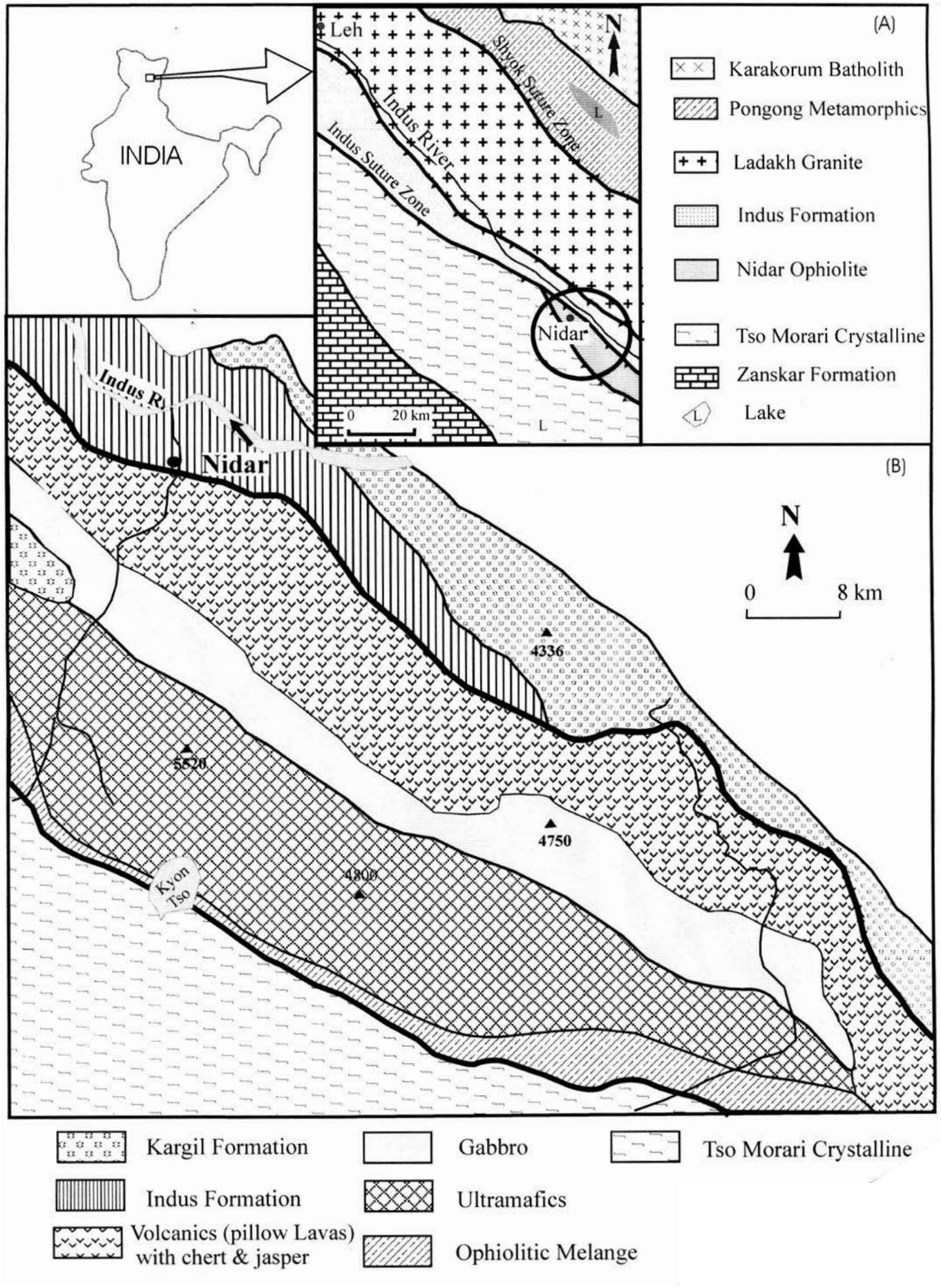

Fig. 1 - Geological map of Nidar ophiolitic sequence (after Thakur and Mishra, 1984).

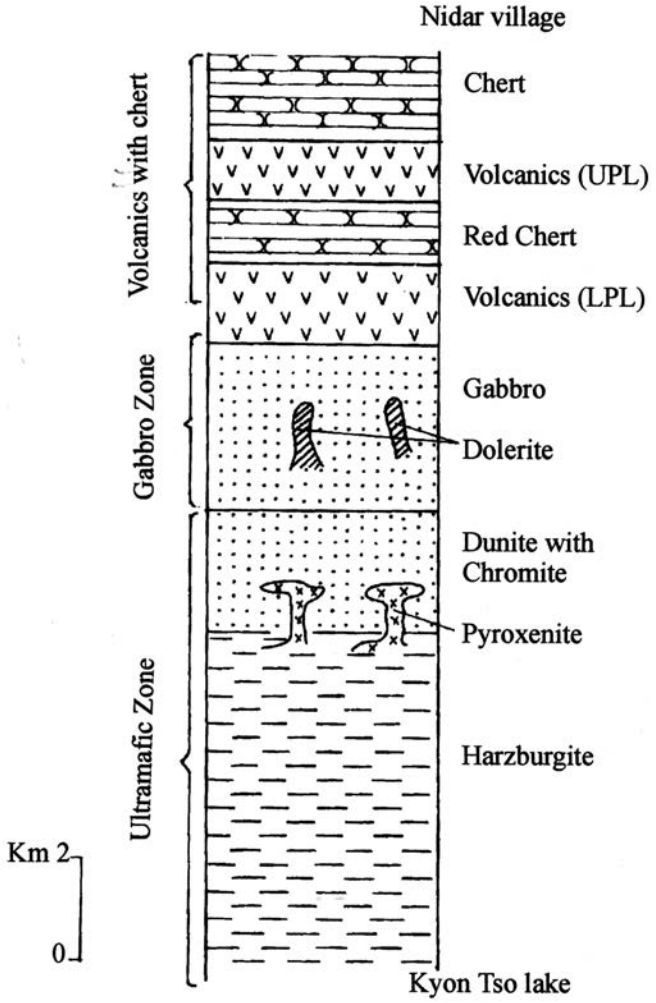

Fig. 2 - Schematic cross-section of Nidar ophiolitic sequence.

PETROGRAPHY

Spinel Harzburgite

The spinel harzburgite suite occupies most part of the ultramafic zone. It consists by 56-89% of olivine, 13-37% of orthopyroxene, 1 to 10% of clinopyroxene and ~7% of Cr-rich spinel. The plagioclase is also noticed in very minor amounts in secondary aggregates. Most of the studied samples have a dominant coarse-grained mosaic texture, with subordinated fine-grained secondary zones. The development of mosaic texture can be reasonably ascribed to recrystallization phenomena after a main melting event and was characterized by the increase of grain size of olivine and orthopyroxene. Olivine crystals are anhedral and equant. The olivine crystals defining the mosaic texture are coarse (up to 15 mm in diameter), and show subgrain boundaries (kink bands). Smaller strain-free olivine crystals (<2 mm across) are instead present in the secondary aggregates, in which they are associated with neoblastic spinel, pyroxenes and minor amount of plagioclase. Similarly to the olivine, the largest orthopyroxene crystals (ª2 mm) show undulatory extinction and exsolution lamellae of clinopyroxene or spinel, whereas the orthopyroxenes from fine-grained aggregates are strain-free. The clinopyroxenes occur as small crystals in the secondary aggregates and are normally associated with interstitial spinel

The spinels are brown and exhibit mainly vermicular shape. Vermicular spinel have irregular grain boundaries, especially at the contact with orthopyroxene and usually enclose small clinopyroxenes. Subhedral to euhedral spinels are sometimes presents in the fine-grained aggregates in association with olivine and pyroxenes. Differently, some spinels occur as rounded, embayed crystals, and usually enclose small olivine crystals. Such textures have been interpreted as a result of corrosion and recrystallization of spinel due to the percolation of the exotic melts (Leblanc, 1980; Lorand and Cottin, 1987).

Spinel Dunite

The olivine-rich rock are equigranular and contain spinel from 2 to 4%, clinopyroxene from 1 to 7% and rare orthopyroxene. The dunite-forming minerals are essentially strain-free, but some elongated olivines are present. Orthopyroxene and clinopyroxene show the same textural features observed in the spinel-harzburgites, even if former is significantly less abundant. The recrystallization into strain-free domain is much common.

The shape of interstitial spinel grains is rounded to vermicular. The vermicular spinel grains show intergrowth with the secondary clinopyroxenes Rounded grains are also observed as inclusions in large olivine. However, similarity to harzburgites, interstitial spinels sometimes contain small olivines, which suggest that both spinel and olivine recrystallized as a consequence of melt percolation.

Pyroxenites

The pyroxenites (websterites) are mainly composed of clinopyroxene which constitutes around 82% of modal composition, and by 10-15% of orthopyroxene, whereas olivine is always less than 7%. Some clinopyroxene aggregates recrystallized into mosaic texture. The clinopyroxene relict is full of spinel exsolution. In some samples, pyroxenes (clinopyroxenes) also show typical magmatic twinning.

MINERAL CHEMISTRY

Minerals were analyzed at the Roorkee University (India) with electron microprobe “Jeol Superprobe” model. The analytical conditions for spot analysis were: 6 s of counting time for each element, and 3 s of counting time for the background, 15 kV of accelerating potential and 15 nA of sample current. Natural and synthetic minerals were used as standards. Data reduction was performed with the ZAF correction procedure.

Olivine

The Fo value and the NiO content are more variable in harzburgite olivine than in dunite olivine (Table 1). The harzburgite olivine has Fo value in the range of 91-94, which is positively correlated with the NiO content (Fig. 3). In particular, the maximum NiO content (0.98%) is shown by the Fo-richest sample. The dunite olivine have Fo in the range of 92.2-92.5, and, therefore, it results enclosed in the compositional range of harzburgite olivine. The NiO content is strictly and positively correlated with the Fo value and is in the range of 0.32-0.41%, which corresponds to the lower values exhibited by harzburgite olivines. The high magnesian composition of olivine reveals its refractory character

Table 1 - Representative analysis of olivines from ultramafic rocks of the Nidar ophiolitic sequence.

sample	NN 47	NN 49	NN 50	NN 51	NN 53	NN 54	NN 56	NN 57	NN 58	NN 59
	Spinel-dunite		Spinel-harzburgite							
SiO2	41,69	41,5	42,65	42,67	42,04	41,45	40,74	40,98	42,42	42,16
Al2O3	0,01	0,01	0,01	-	0,01	0,01	-	-	-	0,01
FeO	7,61	7,24	9,01	5,99	7,94	8,12	6,69	8,86	5,88	6,71
MgO	50,32	49,87	48,05	51,76	50,23	50,93	50,46	50,28	50,42	49,89
MnO	0,67	1,21	0,12	0,04	0,16	0,17	0,01	0,02	0,08	0,07
CaO	0,04	0,04	0,02	-	0,01	0,02	0,14	0,14	0,08	-
TiO2	-	-	0,01	-	-	-	-	-	0,02	-
Cr2O3	-	0,08	0,34	0,11	0,03	-	0,04	0,04	0,09	0,09
NiO	0,32	0,41	0,34	0,64	0,41	0,39	0,94	0,89	0,98	0,92
Total	100,66	100,36	100,55	101,21	100,83	101,09	99,02	101,21	99,97	99,85
Cations										
Si	1,007	1,007	1,032	1,015	1,012	0,998	0,998	0,996	1,022	1,025
Al	0	0	0	-	0	0	-	-	-	-
Fe2 +	0,154	0,149	0,182	0,119	0,16	0,163	0,137	0,18	0,119	0,136
Mg	1,811	1,803	1,733	1,835	1,803	1,828	1,843	1,822	1,819	1,808
Mn	0,014	0,025	0,002	0,001	0,003	0,003	0	0,0004	0,0016	0,001
Ca	0,001	0,001	0,001	-	-	0,001	0,004	0,0003	0,002	
Cr	0	0	0,007	0,002	0,001	-	0,001	0,007	0,001	0,001
Ni	0,006	0,006	0,007	0,012	0,008	0,007	0,019			
Fo	92,2	92,5	93,8	93,9	91,8	91,8	93,1	91	93,8	93

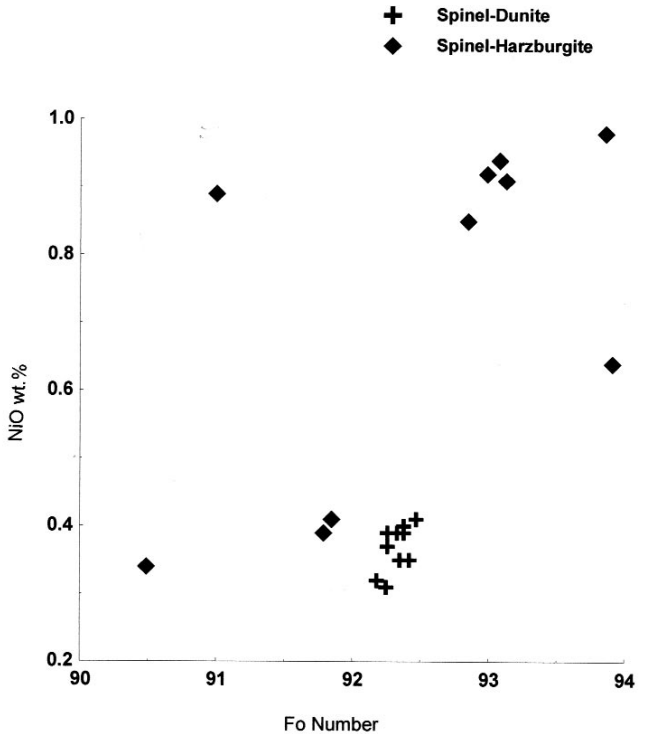

Fig. 3 - NiO vs Fo number in olivine.

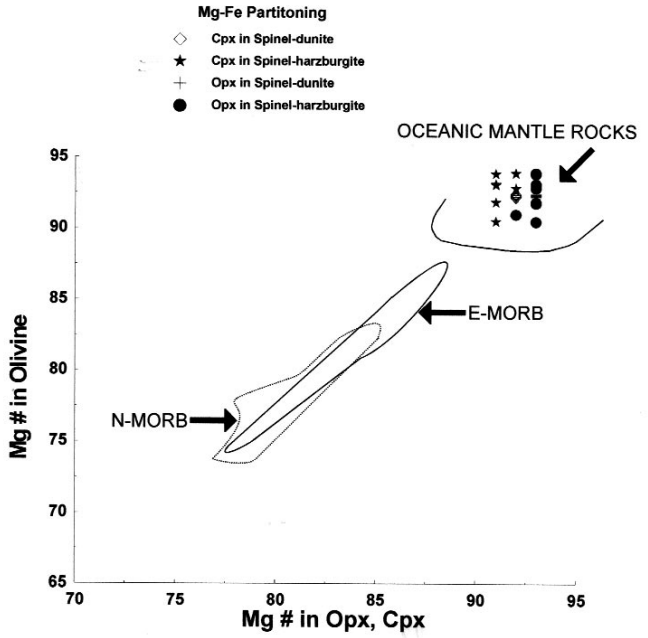

Fig. 4. Fe-Mg partitioning between olivine, orthopyroxene and clinopyroxene from Nidar ultramafics. The field for N-MORB and E-MORB at 1 atm. is taken from Grove and Brian (1983).

similar to that observed in Oman and New Caledonia ophiolite (Auge and Roberts, 1982; Johan and Auge, 1986). The olivines of Nidar ultramafics have typical compositions close to those found in oceanic peridotites and are consistent with a upper mantle origin (Dick and Fisher, 1984). The Mg# of olivine and coexisting clinopyroxene and orthopyroxene are compared in Fig. 4, where field of oceanic mantle rocks is shown. It is significant to notice that Mg# olivines of Nidar ultramafics are similar to those reported for oceanic mantle rocks and higher than those fields defined for comparison such as E-MORB and N-MORB.

Orthopyroxene

The orthopyroxene shows Mg# [cation ratios 100 Mg/(Mg+Fe total)] and Al_2O_3 in the range of 91.2 to 92.0 and 1.01 to 3.4 wt%, respectively (Table 2). In Al_2O_3 vs Mg# plot, the composition of the orthopyroxenes from spinel-harzburgite and pyroxenite are partially comprised within in the field of abyssal peridotite (Fig. 5), but some data of spinel-harzburgite show Al-depleted composition. The Al_2O_3 content in orthopyroxene from dunite shows little variation and is close to the Al-depleted composition of

Table 2 - Representative analysis of orthopyroxene from ultramafic rocks of Nidar ophiolitic sequence.

sample	NN 47	NN 49	NN 50	NN 51	NN 53	NN 54	NN 56	NN 57	NN 58	NN 59	P-9	P-10	P-11	P-12
	Spinel-dunite		Spinel-harzburgite								Pyroxenite			
SiO2	58,56	57,78	59,23	58,28	56,1	57,65	57,86	56,65	59,54	55,68	56,85	57,1	56,76	56,98
Al2O3	1,48	1,31	1,57	1,53	1,38	1,01	2,11	2,85	3,4	3,02	2,67	2,7	2,68	2,89
FeO	5,53	5,49	5,59	5,5	5,37	5,45	5,63	5,53	5,68	5,61	5,35	5,39	5,34	5,36
MgO	33,68	34,18	32,88	33,86	34,58	35,15	32,76	33,48	32,95	33,58	33,91	34,38	33,99	33,98
MnO	0,14	0,13	0,14	0,13	0,1	0,12	0,09	0,1	0,09	0,08	0,14	0,13	0,12	0,12
CaO	0,38	0,49	0,85	0,92	1,1	0,99	0,91	0,95	1,11	1,08	0,56	0,39	0,4	0,5
Na2O	0,08	0,07	-	-	0,06	0,07	0,06	0,06	0,14	0,13	0,01	0,06	0,05	0,04
TiO2	0	0,01	0,02	0,01	0,01	0	0	0,03	0,04	0,04	0,02	0,03	0,03	0,04
Cr2O3	0,48	0,46	0,49	0,51	0,45	0,47	0,46	0,48	0,45	0,44	0,47	0,46	0,49	0,5
NiO	-	-	-	-	-	-	-	-	-	-	0,16	0,12	0,15	0,17
Sum	100,33	99,92	100,81	99,77	99,15	101,21	99,92	100,13	99,66	98,43	100,14	100,16	100,01	100,58
Cations														
Si	1,99	1,97	2,01	1,98	1,923	1,96	1,97	1,94	1,97	1,92	1,95	1,94	1,94	1,94
Al	0,059	0,058	0,062	0,061	0,055	0,04	0,084	0,114	0,132	0,122	0,107	0,108	0,103	0,115
Fe2+	0,157	0,157	0,158	0,156	0,132	0,154	0,16	0,158	0,157	0,161	0,153	0,153	0,153	0,153
Mg	0,928	0,949	0,923	0,938	0,881	0,824	0,758	0,789	0,748	0,812	0,924	0,928	0,924	0,918
Mn	0,004	0,003	0,004	0,003	0,002	0,003	0,002	0,002	0,002	0,002	0,004	0,003	0,003	0,003
Ca	0,013	0,018	0,03	0,033	0,04	0,036	0,033	0,034	0,039	0,039	0,02	0,014	0,014	0,018
Na	0,005	0,004	-	-	0,003	0,004	0,003	0,003	0,009	0,008	0	0,003	0,003	0,002
Ti	-	-	-	-	-	-	-	-	-	-	0	0	0	0,001
Cr	0,012	0,12	0,013	0,013	0,012	0,012	0,012	0,013	0,011	0,012	0,012	0,012	0,013	0,013
Ni	-	-	-	-	-	-	-	-	-	-	0	0	0	0
Mg #	91,55	91,97	91,28	91,63	91,99	91,99	91,19	91,51	91,16	91,44	92,1	92,3	92,4	92,2

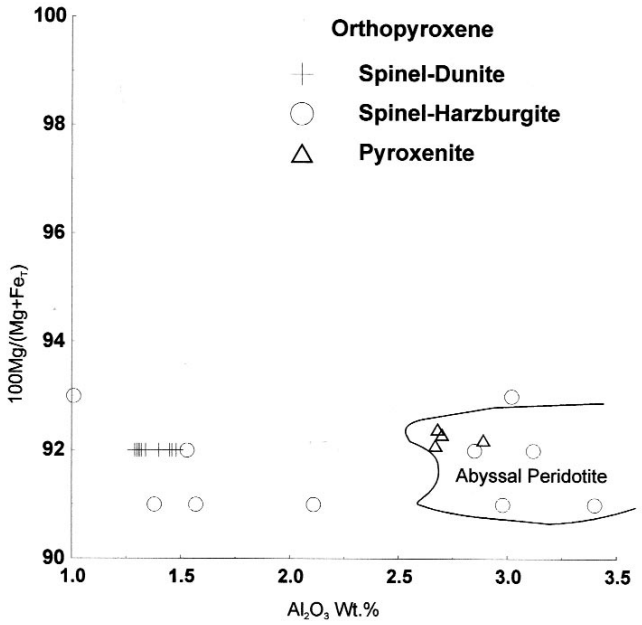

Fig. 5 - Mg # vs wt% Al_2O_3 in orthopyroxene from harzburgite and dunite. The field of abyssal peridotite is after Elthon (1989).

harzburgite orthopyroxene. The Mg# value is nearly constant and within the harzburgite orthopyroxene range.

The CaO in orthopyroxene varies in the range of 0.38 - 1.11 wt%. The Al_2O_3 content in orthopyroxene from dunite is lower than in the orthopyroxene from harzburgite and pyroxenite, while Mg# remains nearly constant. The Al_2O_3 content of orthopyroxenes is similar to the oceanic mantle rocks as described by Hebert et al. (1989). The Al_2O_3 and CaO content are similar to those of Acjoe harzburgite and mantle section of ophiolitic peridotite of Zambales (Evans and Hawkins, 1989). In general, the composition of orthopyroxene from harzburgite and dunite of Nidar ophiolitic sequence is consistent with the highly depleted character of the mineral assemblages.

Clinopyroxene

The Mg# in the diopside from peridotite varies from 91 to 95 (Table 3). The CaO, Al_2O_3 and Cr_2O_3 show consistency in their compositional variation: 23.6-25.96 wt%, 1.24-4.64 wt%, 0.03-0.14 wt%, respectively (Table 3). Na_2O and TiO_2 are present in low to very low concentration. However, Na_2O is significantly higher in pyroxenite clinopyroxenes (0.23-0.30 %) with respect to peridotite clinopyroxene (0.04-0.08%). The Na_2O concentration and Mg# value of the clinopyroxene from pyroxenite are consistent with those reported by Beccaluva et al. (1989) for boninite clinopyroxenes. On the other hand, the low TiO_2 content in clinopyroxene from pyroxenites closely resembles to the clinopyroxene analyzed in intrusive websterites and clinopyroxenites from the Oman, Thetford Appalachian and Thailand ophiolites (Ernewein et al., 1986; Hebert and Laurent, 1989; Orberger et al., 1995), whereas similar low Cr content has been reported for boninite clinopyroxene from Newfoundland ophiolite (Beccaluva et al.,1989; Bedard,1999). In conclusion, all the compositional features of pyroxenite clinopyroxenes (Table 4) suggest that the Nidar cumulates were formed from magmas having boninitic affinity, in a island arc setting.

If the pyroxenite clinopyroxene composition can be assumed to be directed depended from parental melt composition, this is not true for a metasomatic clinopyroxene, on which the peridotite composition plays an important buffering effect. For example looking at the low Ti and Na content of peridotite clinopyroxene, these are consistent with the general depleted character of the ambient peridotite. However, the low Cr composition cannot be inherited from depleted peridotite matrix and it is, therefore, a strong clue that secondary clinopyroxene crystallized in the presence of a SiO_2-and MgO-rich component similar to the parent magma of pyroxenites. The significant compositional similarity occurring between the peridotite and the pyroxenite clinopyroxenes suggests that the former are the product of a large-scale porous flow percolation operated by same melt flowing in the pyroxenite conduits, and that metasomatic clinopyroxene was close to the equilibrium with it.

The Mg# and the total aluminum are negatively correlat-

Table 3 - Representative analysis of clinopyroxene from ultramafic rocks of Nidar ophiolitic sequence.

sample	NN 47	NN 49	NN 50	NN 51	NN 53	NN 54	NN 56	NN 57	NN 58	NN 59
	Spinel-dunite		**Spinel-harzburgite**							
SiO2	53,91	59,28	54,86	59,48	54,78	53,98	53,68	54,35	54,51	54,01
Al2O3	2,18	2,16	2,34	2,11	2,16	2,1	2,13	2,38	2,12	2,13
FeO	2,29	2,26	2,17	2,25	2,2	2,23	2,19	2,58	2,26	2,18
MgO	16,34	15,98	16,82	16,84	16,21	16,81	15,34	15,86	16,41	17,01
MnO	0,07	0,06	0,06	0,08	0,06	0,06	0,07	0,09	0,08	0,07
CaO	24,27	24,82	23,56	23,99	24,08	24,58	24,39	24,79	24,2	24,2
Na2O3	0,07	0,08	0,05	0,04	0,06	0,07	0,06	0,06	0,08	0,07
TiO2	0,06	0,05	0,08	0,09	0,07	0,04	0,07	0,05	0,09	0,08
Cr2O3	0,1	0,12	0,09	0,08	0,09	0,11	0,2	0,1	0,12	0,2
Sum	99,29	99,75	99,73	99,96	99,71	99,98	99,03	99,26	99,9	99,88
Cations										
Si	1,96	2,03	1,979	2,03	1,985	1,96	1,98	1,969	1,971	1,95
Al	0,093	0,087	0,099	0,084	0,092	0,089	0,092	0,1016	0,09	0,191
Fe	0,069	0,064	0,065	0,064	0,066	0,067	0,067	0,077	0,068	0,065
Mg	0,889	0,816	0,904	0,857	0,875	0,909	0,844	0,856	0,886	0,919
Mn	0,002	0,001	0,001	0,002	0,001	0,001	0,002	0,002	0,002	0,002
Ca	0,094	0,911	0,91	0,877	0,935	0,956	0,965	0,962	0,94	0,94
Na	0,004	0,005	0,003	0,002	0,004	0,004	0,004	0,004	0,005	0,004
Ti	0,001	0,001	0,002	0,002	0,001	0,001	0,001	0,001	0,002	0,002
Cr	0,002	0,003	0,002	0,022	0,002	0,003	0,005	0,002	0,003	0,005
Mg #	92,7	92,6	92,7	93	92,9	93	92,5	91,7	92,8	93,31

sample	P-1	P-2	P-3	P-4	P-5	P-6	P-7	P-8
	Pyroxenite							
SiO2	52,84	54,13	53,16	53,18	54,56	53,98	54,98	54,97
Al2O3	4,64	4,31	3,98	4,25	1,24	1,31	2,37	2,36
FeO	3,24	4,17	2,92	3,41	2,39	3,15	3,16	2,16
MgO	12,61	13,28	14,64	15,61	13,98	14,16	15,16	16,13
MnO	0,14	0,16	0,18	0,14	0,14	0,14	0,13	0,14
CaO	20,98	25,31	24,58	23,96	25,96	25,61	24,96	25,96
Na2O	0,23	0,27	0,29	0,3	0,028	0,27	0,23	0,24
TiO2	0,04	0,06	0,07	0,06	0,03	0,02	0,02	0,03
Cr2O3	0,04	0,03	0,04	0,01	0,11	0,14	0,08	0,08
NiO	0,01	0,01	0,01	0,01	0,01	0,01	0,01	0,01
Sum	98,77	101,73	99,87	100,93	98,7	98,79	101,1	120,08
Cations								
Si	1,94	1,94	1,93	1,92	2,01	1,998	1,98	1,96
Al total	0,201	0,182	0,171	0,18	0,053	0,057	0,1	0,099
Fe	0,099	0,125	0,089	0,102	0,073	0,097	0,095	0,064
Mg	0,693	0,711	0,795	0,84	0,769	0,781	0,813	0,875
Mn	-	-	0,002	-	-	-	-	-
Ca	0,987	0,975	0,96	0,926	1,026	1,016	0,963	0,991
Na	0,016	0,018	0,02	0,021	0,02	0,019	0,016	0,016
Ti	0,001	0,001	0,001	0,001	0	0	0	0,001
Cr	0,001	0,0008	0,001	0	0,003	0,004	0,002	0,002
Ni	0,002	0	0	0	0	0	0	0
Mg #	87,4	85,1	90,4	89,4	91	89,2	90,4	93,3

Table 4 - Representative analysis of Cr-spinel from ultramafic rocks of Nidar ophiolitic sequence.

sample	NN 47	NN 49	NN 50	NN 51	NN 53	NN 54	NN 56	NN 57	NN 58	NN 59	P 1	P 2	P 3	P 4
	Spinel-dunite		**Spinel-harzburgite**								**Pyroxenite**			
FeO	28,22	25,12	22,07	23,08	28,68	26,78	27,34	28,16	25,78	26,98	21,98	18,78	20,98	21,64
TiO2	0,04		0,01	0,03	0,02	0,02	0,02	0,03	0,03	0,02	0,01	0,02	0,01	0,03
MgO	9,61	9,4	11,88	12,84	10,84	9,78	8,28	7,28	9,86	8,85	11,62	12,84	13,64	14,67
Al2O3	10,65	10,69	19,97	18,76	10,66	10,86	10,24	9,16	11,26	10,12	10,42	14,97	10,97	10,74
MnO	0,52	0,64	0,25	0,28	0,52	0,62	0,76	0,68	0,56	0,68	0,3	0,29	0,28	0,3
Cr2O3	50,01	53,26	44,35	45,75	50,08	52,84	52,81	53,76	51,58	52,65	54,86	52,74	53,74	52,28
ZnO	0,22	0,14	0,2	0,17	0,14	0,16	0,11	0,1	0,14	0,2	0,1	0,02	0,02	0,01
Sum	99,28	99,28	98,73	100,91	100,93	101,06	99,55	99,17	99,21	99,4	99,39	99,81	99,71	99,74
Cations														
Fe+2	0,508	0,514	0,431	0,398	0,461	0,506	0,564	0,611	0,497	0,537	0,426	0,379	0,343	0,299
Fe+3	0,273	0,183	0,15	0,197	0,313	0,222	0,199	0,188	0,214	0,214	0,174	0,285	0,651	0,276
Ti	0	-	-	-	-	-	-	-	-	-	-	-	-	-
Mg	0,474	0,465	0,558	0,591	0,522	0,474	0,412	0,368	0,484	0,439	0,566	0,613	0,651	0,695
Al	0,415	0,418	0,742	0,683	0,405	0,416	0,403	0,366	0,437	0,397	0,401	0,372	0,414	0,402
Mn	0,014	0,017	0,006	0,007	0,014	0,017	0,021	0,019	0,015	0,019	0,008	0,007	0,007	0,008
Cr	1,308	1,397	1,1	1,117	1,279	1,359	1,39	1,443	1,34	1,38	1,418	1,337	1,367	1,315
Zn	0,005	0,003	0,004	0,003	0,003	0,003	0,002	0,002	0,003	0,004	0,002	-	-	-
Cr #	75,91	76,97	59,81	62,08	76,02	76,54	77,56	79,96	73,44	77,71	78,25	77,9	76,75	76,58
Fe3+ #	14,18	13,33	9,85	10,69	14,32	13,56	12,18	13,69	13,21	13,27	14,32	8,7	26,7	13,84
Mg #	48,85	52,07	59,51	60,84	51,37	48,57	44,47	41,79	52,42	50	40	48	39	41,44

ed, and this is especially clear for pyroxenite clinopyroxene (Fig. 6). The TiO_2 and Al^{IV+VI} show positive correlation in pyroxenite but not in the peridotites (Fig. 6a). The variation in pyroxenitic clinopyroxenes are consistent with magmatic differentiation, whereas the Mg# and Al in harzburgite clinopyroxene seems to be buffered by peridotitic composition. As a whole, the Figs. 6a and 6b also shows that Nidar clinopyroxenes are more akin to boninitic than to ophiolitic clinopyroxenes.

The comparison of the compositions of clinopyroxene and orthopyroxene can give important insights in the recrystallization process of the peridotites. From the data reported in Tables 2 and 3, it is evident that in the pyroxenes from peridotite, the Cr_{Cpx}/Cr_{Opx} ratios are surprisingly lower than 1, whereas Al_{Cpx}/Al_{Opx} ratios are higher as well as lower than 1. Beccaluva et al. (1989) suggests that similar variable Al_{Cpx}/Al_{Opx} ratios may be due to the presence of a wide range of thermochemical regime. However, such a compositional ratios can be simply explained by the occurrence of chemical disequilibrium between newly-formed peridotite clinopyroxenes and deformed orthopyroxenes, that are residual after the partial melting event(s). The presence of same compositional features in pyroxene pairs from pyroxenites suggest that most (or all) the orthopyroxenes in the pyroxenite bands are metamorphic rather than magmatic, or than those orthopyroxenes have crystallized before clinopyroxene in equilibrium with a more primitive (Si-and Cr-enriched) magma.

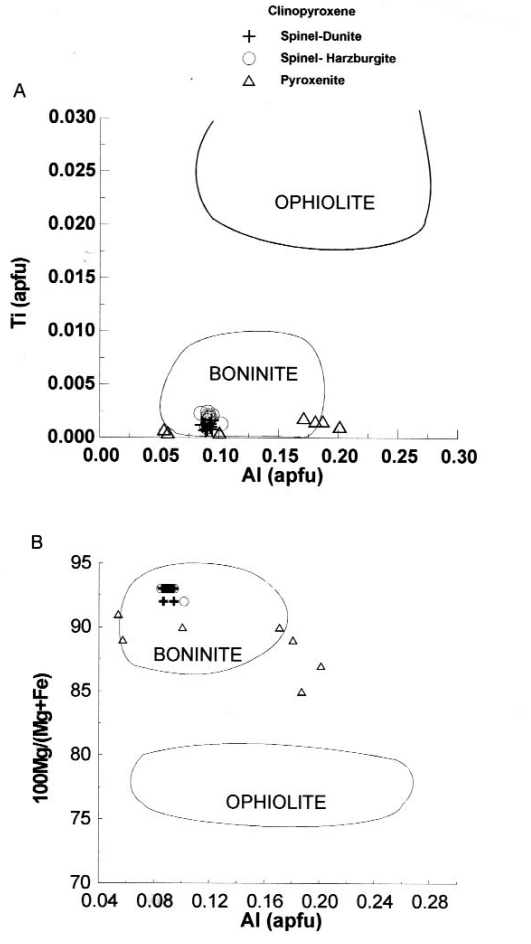

Fig. 6 - Chemical composition of clinopyroxene in dunite and harzburgites. (a) Ti vs Al^{iv+vi} (b) Mg/(Mg+Fe) vs Al^{iv+v}. The data for ophiolitic and boninitic clinopyroxene is after Beccaluva et al. (1989).

Spinel

Peridotite spinel has chromite to Mg-chromite composition with Mg# in the range 41-60, while Cr# varies from 59 to 79 (Table 5). The spinels have very low TiO_2 concentration (up to 0.04 wt%). The spinels of pyroxenite also exhibits low TiO_2 (0.03 wt.%). Cr# values range from 76 to 78, while Mg# varies from 39 to 48 (Table 5) The TiO_2 wt% vs Cr# plot (Fig. 7) reveals that chromite component in peridotite spinels are significantly higher than that caused by high-degree pf partial melting processes. Such a composition is more consistent with crystallization via peridotite-melt interaction (Zhou et al., 1996), according to the textural occurrence of peridotite spinel in neoblastic zones and clinopyroxene compositions. In the Fig. 7, most of the peridotite spinels and all the pyroxenite spinels plot together in the boninitic field. This observation is consistent with the consideration on clinopyroxene compositions done in the previous paragraphs, and as a whole support the hypothesis that the melt percolating the peridotite was the same documented by pyroxenite zone, having boninitic affinity.

A further striking feature of the peridotite assemblages is that the Cr_{Sp}/Cr_{Cpx} values are exceptionally high notwithstanding, the texture equilibrium evidenced by such phases. The anomalous values can be explained by the stability of the plagioclase in the secondary aggregates or by particular combination of melt composition and intensive parameter conditions. For example, it is also consistent with the occurrence of the percolation at low P, under plagioclase-facies conditions of peridotite system. The low TiO_2 content in Cr-spinel is also observed from well established boninitic parentage of New Caledonia and Papua New Guinea ophiolites (Jaques and Chapell, 1980; Leblanc, 1985). The wide variation in Mg# probably reflects subsolidus re-equilibration of Fe-Mg partitioning with their host olivine.

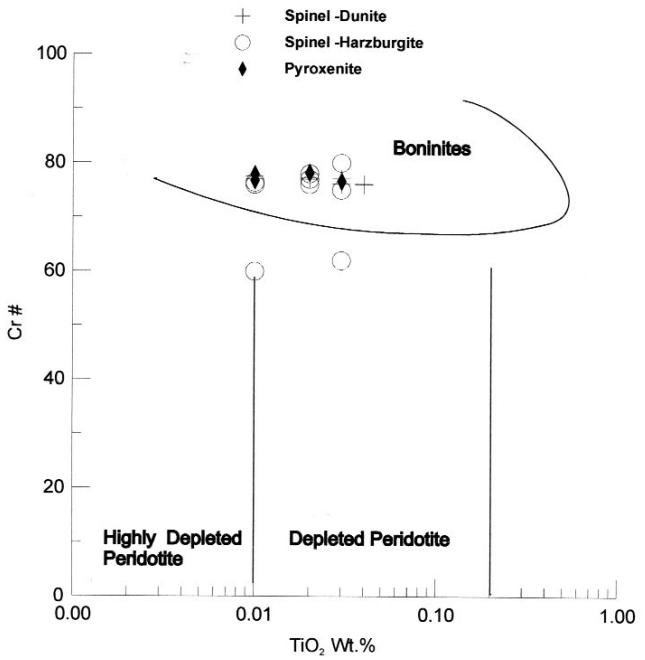

Fig. 7 - TiO_2 (wt%) vs Cr/(Cr+Al) are compared with spinels from boninites (after Arai, 1992) and depleted and highly depleted peridotite (after Jan and Windley, 1990).

Table 5 - Chemical composition of pyroxene from pyroxenites

sample	P-1	P-2	P-3	P-4	P-5	P-6	P-7	P-8	P-9	P-10	P-11	P-12
SiO2	52,84	54,13	53,16	53,18	54,56	53,98	54,98	54,97	56,85	57,1	56,76	56,98
Al2O3	4,64	4,31	3,98	4,25	1,24	1,31	2,37	2,36	2,67	2,7	2,68	2,89
FeO	3,24	4,17	2,92	3,41	2,39	3,15	3,16	2,16	5,35	5,39	5,34	5,36
MgO	12,61	13,28	14,64	15,61	13,98	14,16	15,16	16,13	33,91	34,38	33,99	33,98
MnO	0,14	0,16	0,18	0,14	0,14	0,14	0,13	0,14	0,14	0,13	0,12	0,12
CaO	20,98	25,31	24,58	23,96	25,96	25,61	24,96	25,96	0,56	0,39	0,4	0,5
Na2O	0,23	0,27	0,29	0,3	0,028	0,27	0,23	0,24	0,01	0,06	0,05	0,04
TiO2	0,04	0,06	0,07	0,06	0,03	0,02	0,02	0,03	0,02	0,03	0,03	0,04
Cr2O3	0,04	0,03	0,04	0,01	0,11	0,14	0,08	0,08	0,47	0,46	0,49	0,5
NiO	0,01	0,01	0,01	0,01	0,01	0,01	0,01	0,01	0,16	0,12	0,15	0,17
Sum	98,77	101,73	99,87	100,93	98,7	98,79	101,1	120,08	100,14	100,16	100,01	100,58
Cations												
Si	1,94	1,94	1,93	1,92	2,01	1,998	1,98	1,96	1,95	1,94	1,94	1,94
Al total	0,201	0,182	0,171	0,18	0,053	0,057	0,1	0,099	0,107	0,108	0,103	0,115
Fe	0,099	0,125	0,089	0,102	0,073	0,097	0,095	0,064	0,153	0,153	0,153	0,153
Mg	0,693	0,711	0,795	0,84	0,769	0,781	0,813	0,875	0,924	0,928	0,924	0,918
Mn	-	-	0,002	-	-	-	-	-	0,004	0,003	0,003	0,003
Ca	0,987	0,975	0,96	0,926	1,026	1,016	0,963	0,991	0,02	0,014	0,014	0,018
Na	0,016	0,018	0,02	0,021	0,02	0,019	0,016	0,016	0	0,003	0,003	0,002
Ti	0,001	0,001	0,001	0,001	0	0	0	0,001	0	0	0	0,001
Cr	0,001	0,0008	0,001	0	0,003	0,004	0,002	0,002	0,012	0,012	0,013	0,013
Ni	0,002	0	0	0	0	0	0	0	0	0	0	0
Mg #	87,4	85,1	90,4	89,4	91	89,2	90,4	93,3	92,1	92,3	92,4	92,2

DISCUSSION

As a whole, the composition of the minerals of the tectonic ultramafics from Nidar shows that they represent pieces of ancient abyssal peridotite, which experienced a multi-stage evolution involving partial melting episode(s) and large-scale porous flow melt percolation. Refractory peridotites (harzburgites and dunites) are found in the oceanic margin or continental lithospheric mantle and are normally interpreted the resultant product of high degree of partial melting (Dick and Bullen, 1984; Bodineir, 1988; Johnson and Dick, 1992).

The melting of 42% of MORB pyrolite mantle is required to have Cpx-free harzburgite, while >60% of melting must occur to have Opx-free dunite (Kostopoulos, 1991). In the study area, the content of Cpx in the most fertile peridotites is lower than 10%, while the dunite has orthopyroxene in traces. According to Kostopoulos (1991), 10 to 40% of partial melting of pyrolite mantle may be responsible for the observed modal composition of minerals in Nidar harzburgites. Niu (1997) suggested that this type of peridotite is the mixture of melting residue and excess olivine crystallize in response to decompression melting. On the other hand, the mineral chemistry (e.g. the lower Mg# of dunite olivines with respect to those of most harzburgite olivines) evidences that Nidar dunites cannot simply be the product of higher degree of partial melting starting from common source. A large number of textural and chemical features show that pervasive porous flow percolation occurred in both harzburgite and dunite after the partial melting event(s). This occurrence points to the possibility that dunite mineral assemblage was determined by an intense reaction between the ambient harzburgite and an uprising melts. If the peridotite-melt reaction occurred at temperature lower than peridotite solidus, the significant decrease of the modal volume of orthopyroxene in dunite requires that the melt was SiO_2-undersaturated. Differently, if the melt was SiO_2-saturated (as suggested by the chemistry of fine-grained secondary aggregates, which are formed by clinopyroxene+Cr-spinel+olivine+orthopyroxene+plagioclase), partial melting had to occur to determine the extreme decrease of the orthopyroxene content recorded by dunites. A further model could to envisage an early percolation of a SiO_2-undersaturated melts that in the final stage becomes SiO_2-saturated, via orthopyroxene dissolution.

Anyway, the percolation process determined the nearly complete recrystallization of the uppermost level of the Nidar sequence producing dunite. On the basis of the texture and chemical evidences the following events can be recognized: 1) high-degree partial melting process(es), which virtually determined the complete consumption of clinopyroxene; 2) plastic deformation of the residual mineral assemblages, that can be possibly related to the crustal accretion. The lacking of low-temperature hydrothermal alteration in the tectonic peridotites shows that they escaped the emplacement in the sea-floor environment; 3) late interaction with melts coming from deeper mantle level. Because of the pervasive character of such a percolation and the close correspondence of the major element composition of peridotite and pyroxenite minerals, it is reasonable hypothesized that the pyroxenite conduits represented shear zone where the melt was accumulated, rather than the starting point of the percolation. Similar peridotite-pyroxenites relationships have been suggested to occur in highly-metasomatized subcontinental ultramafic sequences related to mantle wedge from Western Alps (Zanetti et al., 1999).

The compositional features of the pyroxenite clinopyroxene (in particular, the low Ti and Na contents, and the high Mg content) confidently indicate that the percolating melt had boninitic affinity. The same indication is furnished by the large chromite component of the pyroxenite spinels (Fig.7), even if we are not able to assess how much the subsolidus equilibria may have influenced their compositions. However, the considerable homogeneity of the Cr# value of the spinels in the peridotites and pyroxenites from Nidar ophiolite, suggests that their compositions were close to the equilibrium with the percolating melt. The Cr# of spinel >60 are typical of boninitic basalts in island arc environment (Dick and Bullen,1984).

Such types of Cr spinels were also reported from arc re-

lated ophiolitic complex (Ozawa, 1988). The low TiO_2 character of pillow lavas (T. Ahmad, personal communication), which lie above gabbro unit, also supports island arc environment. As a whole, the basaltic melt sequence of Nidar ophiolites is similar to the Troodos ophiolites (Robinson et al., 1983; Mehegan and Robinson, 1991).

In conclusion, the ophiolitic sequence of Nidar area can be considered similar to the ophiolitic sequence with highly-depleted peridotites having magmatism of boninitic affinity recognized in modern oceanic arc system (Bloomer, 1983). As a consequence, the Nidar ophiolites were probably formed in forearc basin related to a supra-subduction zone environment. The absence of pyroclastic rocks and sheeted dyke complex in Nidar also favours a forearc setting and similar type of phenomena was suggested by Robinson et al. (1983) for Troodos ophiolitic complex. Therefore, the described mineralogical, geochemical and geological characteristics suggest a strong affinity to the well- established supra subduction zone ophiolites (Elthon, 1991; Pearce, 1991; Roberts, 1992).

CONCLUSIONS

The mineralogical and chemical study of ultramafic rocks from Nidar ophiolitic sequence has revealed various petrochemical processes that occurred in the upper mantle during Cretaceous. The following conclusions can be drawn for the genesis of ultramafic rocks of Nidar ophiolitic sequence.

1. Ultramafics (harzburgites and dunites) rocks of Nidar ophiolitic sequence are highly refractory in character mainly related to partial melting phenomena.
2. The chemical composition of minerals present in the ultramafic rocks reveals that a percolating melt reacted with peridotite after melting episodes. Such a melt was rich in MgO, but poor in Al_2O_3, CaO and TiO_2 indicating boninitic affinity within island arc setting. The melt/peridotite interaction probably produced clinopyroxene-bearing spinel-dunite.
3. As a whole, petrographic and mineral chemistry data suggest that the ultramafic rocks of Nidar ophiolite are formed in the fore-arc setting of supra subduction tectonic environment.

Acknowledgements

I am thankful to the Dr. N.S. Virdi, Director of Wadia Institute of Himalayan Geology, Dehra Dun, for his constant encouragement during the progress of this work and to Drs. T. Ghosh and M. Manikvasagam for providing the EPMA facilities at Roorkee University. I am also indebted with the Dr. Cs. Szabo and Prof. E. Neumann for reviewing an initial version of the manuscript. Author is also highly grateful to Dr. A. Zanetti, reviewer of the Journal for giving good suggestions for the all-round improvement of the manuscript.

REFERENCES

Andersen T., O'Reilly S.Y. and Griffin W.L., 1984. The trapped fluid phase in upper mantle xenoliths from Victoria, Australia: implication for mantle metasomatism. Contrib. Mineral. Petrol., 86: 72- 85.

Auge T. and Roberts S., 1982. Petrology and geochemistry of some chromitiferous bodies within the Oman ophiolite. Ofioliti, 7: 133-154.

Beccaluva L.and Serri G.C., 1988. Boninitic and low Ti subduction related lavas from intra-oceanic arc backarc system and low Ti ophiolites: a reappraisal of their petrogenesis and original tectonic setting. Tectonophysics, 146: 291- 315.

Beccaluva L., Macciotta G., Piccardo G.B. and Zedce O., 1989. Clinopyroxene composition of ophiolite as a petrogenetic indicator. Chem. Geol., 77. 165-182.

Bedard J.H., 1999. Petrogenesis of boninites from the Betts Cove Ophiolite, Newfoundland, Canada: Identification of subducted source composition. J. Petrol., 40: 1853-1889.

Bodinier J.L., 1988. Geochemistry and petrogenesis of the Lanzo peridotite body, western Alps. Tectonophysics, 149,:67-88.

Bloomer S.H., 1983. Distribution and origin of igneous rocks from the landward slopes of the Mariana trench: implication for its structure and evolution. J. Geophys. Res., 88: 7411- 7428.

Dick H.J.B. and Fisher R.L., 1984. Mineralogic studies of the residues of mantle melting abyssal and Alpine type peridotites. In: J. Kornprobst (Ed.), Kimberlites II, the mantle and crust mantle relationship, Elsevier, Amsterdam, p. 295- 308.

Dick H.J.B. and Bullan T., 1989. Chromian spinel as a petrogenetic indicator in abyssal and alpine type peridotites and spatially associated lavas. Contrib. Mineral. Petrol., 86: 54-76.

Elthon D., 1989. Pressure of origin of primary mid ocean ridge basalts. In: A.D. Saunders and M.J. Norry (Eds.), Magmatism in ocean basins. Geol. Soc. London Spec. Publ., 42: 125 -136.

Elthon D., 1991. Geochemical evidence for the formation of Bay of Island ophiolite above a subduction zone. Nature, 354: 140-143.

Ernewein M., Pflumio C. and Whitechurch H., 1988. The death of an accretion zone as evidenced by the magmatic history of the Semail Ophiolite (Oman). Tectonophysics, 151: 247- 274.

Evans C. and Hawkins J.W., 1989. Compositional heterogeneities in upper mantle peridotites from the Zambales range ophiolite, Luzon, Philippines. Tectonophysics, 168: 23-41.

Greenbaum D., 1977. The chromitiferous rocks of the Troodos ophiolite complex, Cyprus. Econ. Geol., 72: 1175-94.

Griffin W.L., Wass S.Y. and Hollis J.D.,1984. Ultramafic xenoliths from Bullenmerri and Gnotuk mars, Victoria, Australia: Petrology of a sub continental crust mantle transition. J. Petrol., 25: 53- 87.

Grove T.L. and Brian W.B. 1983. Fractionation of pyroxene-phyric MORB at low pressure: An experimental study. Contrib. Mineral. Petrol., 84: 293-309.

Hebert R. and Laurent R., 1989. Mineral chemistry of ultramafic and mafic plutonic rocks of the Appalachian ophiolites, Quebec, Canada. Chem. Geol., 77: 265 -285.

Hebert R., Serri G. and Hekinian R. 1989. Mineral chemistry of ultramafic tectonites and ultramafic to gabbroic from the major oceanic basins and northern Apennine ophiolites (Italy). A comparison. Chem. Geol., 77: 183-207.

Honegger K., Dietrich V., Frank W., Gansser A., Thoni M. and Trommosdorf V., 1982. Magmatism and metamorphism in the Ladakh Himalaya (the Indus Tsangpo suture zone). Earth Planet. Sci. Lett., 60: 253- 292.

Honegger K., Le Fort P., Mascle G. and Zimmermann J.L., 1989. The blueschist along the Indus Suture zone in Ladakh, NW Himalaya. J. Metam. Geol., 7: 57-72.

Jan M.Q. and Windley B.F., 1990. Chromian spinel silicate chemistry in ultramafic rocks of the Jijal complex, northwest Pakistan. J. Petrol., 31: 667 -715.

Jaques A.L. and Chapell B.W., 1980. Petrology and trace element geochemistry of the Papuan ultramafic belt. Contrib. Mineral. Petrol., 75: 55-70.

Johnson K.J.T.M. and Dick H.J.B., 1992. Open system melting and temporal and spatial variations in peridotites and basalts at the Atlantis II fracture zone. Jr. Geophys. Res., 97: 9219-9241.

Johan Z. and Auge T., 1986. Ophiolitic mantle sequences and their evolution mineral chemistry constraints. In: M.J. Galagher, R.A., Ixer, C.R. Neary and H.M. Prichard (Eds.), Metallogeny of basic and ultrabasic rocks. Inst. Min. M. London, p. 305-317.

Kelemen P.B., Dick H.J. and Cuick J.E. 1992. Formation of

harzburgite by pervasive melt rock reaction in the upper mantle. Nature, 358: 635-644.

Kostopoulas D.K., 1991. Melting of the shallow upper mantle: A new perspective. J. Petrol., 32: 671-699.

Leblanc M., 1980. Chromite growth, dissolution and deformations from morphological point of view. SEM investigation. Miner. Deposita., 15: 201-210.

Leblanc M., 1985. Les gisements de spinelles chromifères. Bull. Mineral., 108: 587-602.

Lorand J.P. and Lothin J.Y., 1987. Na-Ti-Zr-H_2O rich mineral inclusions indicating postcumulus chrome-spinel dissolution and recrystallization in the western Laouni mafic intrusion (Algeria). Contrib. Mineral. Petrol., 97: 251-265.

Mehegan J.M. and Robinson P.T.,1991. Lava groups and volcanic stratigraphy of the CCSP boreholes CY 1 and CY 1A, Troodos ophiolite, Cyprus. In: I.L. Gibson, J. Malpas, P.T. Robinson and C. Xenophontos (Eds.), Cyprus crustal study project, Initial report, 4 ,CX 1, and 1t. Geol. Surv. Canada Pap. 90, 20: 177-185.

Molner P. and Tapponier P., 1975. Cenozoic tectonics of Asia: effects of continental collision. Science, 189: 419- 426.

Nicolas A., Bouchez J.L., Boudier F. and Mercier J.C. 1971. Textures, structures and fabrics due to solid state flow in some European lherzolites. Tectonophysics, 12: 55-86.

Nisbet E.G. and Fearce J.A., 1977. Clinopyroxene composition of mafic lavas from different tectonic settings. Contrib. Min. Petrol., 63: 161-173.

Niu,. 1997. Mantle melting and melt extraction processes beneath ocean ridges: Evidence from abyssal peridotite. J. Petrol., 38: 1047-1074.

Ohnenstetter M., Bechon F. and Ohnenstetter D., 1990. Geochemistry and mineralogy of lavas from the Arakapas fault belt, Cyprus: consequences for magma chamber evolution. Mineral. Petrol., 41: 105-124.

Olafsson M. and Eggler D.H.,1983. Phase relations of amphibole, amphibole carbonate and phlogopite carbonate peridotite: petrologic constraints on the asthenosphere. Earth Planet. Sci. Lett., 64: 304-315.

Orberger B., Lovand J.P., Girardeau J., Mercier J.C.C. and Pitragool S., 1995. Petrogenesis of ultramafic rocks and associated chromitites in the Nan Uttaradit ophiolite, Northern Thailand. Lithos, 35: 153-182.

Ozawa K. ,1988. Ultramafic tectonites of the Miyamori ophiolitic complex in the Kitakami mountains, northeast Japan: Hydrous upper mantle in an island arc. Contrib. Miner. Petrol., 99: 159-175.

Pearce J. ,1991. Ocean floor comes ashore. Nature, 354:110-111.

Robinson P.T., Melson W.G., O'Hean T. and Schonincke H.V., 1983. Volcanic glass composition of the Troodos ophiolite, Cyprus, Geology, 11: 400-404.

Roberts S., 1992. Influence of the partial melting regime on the formation of ophiolitic chromitite. In: L.M. Parson, B.J. Murton and P. Browning (Eds.), Ophiolites and their modern oceanic analogues. Geol. Soc. London Spec. Publ., 60: 203 -217.

Sack R.O. 1982. Spinel as petrogenetic indicators: activity composition relation at low pressure. Contrib. Mineral. Petrol., 79: 169- 186.

Takahasi E. and Kushiro I., 1983. Melting of a dry peridotite at high pressures and basalt magma genesis. Am. Mineral., 68: 859 -879.

Thakur V.C., 1981. Regional framework and geodynamic evolution of the Indus Tsangpo suture zone in the Ladakh Himalaya. Trans. Roy. Edinburgh, Earth. Sci., 72: 89-97.

Thakur V.C. and Mishra D.K., 1984. Tectonic framework of the Indus and Shyok suture zones in eastern Ladakh, northwest Himalaya. Tectonophysics, 101: 207-220.

Virdi N.S., 1986. Indus Tsangpo suture in the Himalaya: crustal expression of a palaeo subduction zone. Ann. Soc. Geol. Poloniae., 56: 3- 31.

Zanetti A., Mazzucchelli M., Rivalenti G. and Vannucci R., 1999. The Finero phlogopite-Peridotite massif: An example of subduction-related metasomatism. Contrib. Mineral. Petrol., 134: 107-122.

Zhou M.F., Robinson P.T. and Malpas J. and Li Z., 1996. Podiform chromitites in the Luobusa ophiolite (Southern Tibet): Implications for melt-rock interaction and chromite segregation in the upper mantle. J. Petrol. 37: 3-21.

Received, February 19. 1999
Accepted, May 24, 2001